

EASR**Engineering and Applied Science Research**<https://www.tci-thaijo.org/index.php/easr/index>

Published by the Faculty of Engineering, Khon Kaen University, Thailand

Potential approach to assess seawater breakthrough using attenuated total reflectance-Fourier transform infrared spectroscopyHauwa A. Rasheed^{*1, 2)} and Adekunle A. Adeleke^{2, 3)}¹⁾Department of Industrial Chemistry, Nile University of Nigeria, Jabi, Abuja Federal Capital Territory, Nigeria²⁾Waste to Wealth Research Group, Nile University of Nigeria, Jabi, Abuja Federal Capital Territory, Nigeria³⁾Department of Mechanical Engineering, Nile University of Nigeria, Jabi, Abuja Federal Capital Territory, Nigeria

Received 19 August 2024

Revised 7 March 2025

Accepted 14 March 2025

Abstract

Seawater is commonly utilized as the primary source of water injected into reservoirs as part of secondary recovery operations within oilfields, aiming to optimize production levels. Nevertheless, the implementation of such a procedure can bring about significant issues, such as the formation of sulphate scale, which may arise due to variations in composition between seawater and water present in the reservoir. Consequently, a prompt and straightforward methodology has been devised, leveraging attenuated total reflectance Fourier transform infrared spectroscopy (ATR-FTIR), to supervise the chemical composition of the produced water for any potential signs of seawater breakthrough and to approximate the proportion of seawater present. Through the application of this method, the concentration of sulfate ions (SO_4^{2-}) known to be the primary factor responsible for scale formation, can be accurately determined within the produced water. The evaluation of SO_4^{2-} concentration in both synthesized and true seawater obtained from the shores of Aberdeen, Scotland revealed respective values of 2776 mg/L and 2834 mg/L whereas the detection limit (DL) and the quantification limit (QL) were 50 ppm and 100 mg/L, respectively. The approximated DL for SO_4^{2-} in both synthetic seawater fraction and natural seawater fraction stands at 100 mg/L for each, corresponding to a composition of 5% seawater and 95% formation water. Conversely, its QL is approximated to be 414 mg/L and 500 mg/L, respectively, aligning with compositions of 10% seawater and 90% formation water. Notably, the addition of supplementary ions within the water samples has no impact on the instrument's discernment regarding identifying and quantifying the amount of SO_4^{2-} present. Finally, by plotting the correlation between the actual and measured concentrations, a strong relationship between the two sets of data was uncovered, affirming the potential of FTIR as a rapid, uncomplicated, reliable, and cost-effective approach for evaluating seawater breakthrough occurrences.

Keywords: Oilfield scales, Seawater breakthrough, ATR-FTIR, Calibration**1. Introduction**

The primary activities carried out by oil-producing industries revolve around the intricate operations involved in the production phase within the specific boundaries of an oilfield's development. Each production company is fully aware of the substantial financial investments required for the exploration and advancement of a new oilfield. The overarching objective of such companies is to effectively and efficiently extract oil from the reservoir in a financially viable manner, aiming to maximize the recovery potential [1]. However, the reliance solely on the primary depletion reserves has long ceased to be a sustainable approach. This shift is primarily due to the inherent limitations of such reserves in terms of providing the necessary energy to extract a significant portion of the oil reserves present in the fields [2]. Upon the discovery and development of an oil well, the initiation of production activities triggers a disturbance in the equilibrium of pressure within the reservoir. This disruption prompts the natural forces inherent in the reservoir, to exert pressure on the oil, thereby facilitating its movement towards the production zone [3]. Consequently, over the operational lifespan of an oil well, the reservoir pressure experiences a considerable decline. As time progresses, the feasibility of maintaining a sustainable level of oil production diminishes, potentially resulting in the abandonment of the well despite the substantial remaining oil reserves within the reservoir. Research findings indicate that only a fraction, specifically one-third, of the oil present in reservoirs worldwide is successfully recovered through primary recovery methods [3, 4].

In such scenarios characterized by declining reservoir pressure and diminishing oil production rates, secondary recovery techniques, known as pressure-building operations, are implemented to mitigate these challenges and optimize oil production [5]. These secondary recovery methods encompass a range of approaches, including water injection, steam flooding, and CO_2 injection, among others. The strategic deployment of these operations is deemed more economically prudent and less risky compared to embarking on the exploration of a new oilfield [6]. Notably, among the array of secondary recovery methods, water injection stands out as the most prevalent technique owing to its widespread availability, operational simplicity, efficiency, and cost-effectiveness [7]. Among the available sources for injection into the reservoir, seawater emerges as the most practical due to its widespread availability and abundance. However, it is important to recognise that the composition of the water accessible for injection differs from that of the reservoir's main water [8]. When a breakthrough happens, the preexisting mismatch between the two types of water makes everything challenging [9].

*Corresponding author.

Email address: hauwaRM@outlook.com

doi: 10.14456/easr.2025.26

The phenomenon wherein water or gas put into the reservoir successfully reaches one or more of the producing wells is referred to as a "breakthrough." [10]. This is a crucial event in the oil recovery process since water is also being withdrawn from the formation at the same time. In particular, after seawater seeps through, it is essential to keep an eye on the produced water at all times. This monitoring serves as a vital tool in determining the appropriate course of action, whether it involves initiating scale mitigation strategies or altering the treatment methodology. Seawater is distinguished by its high sulfate ion (SO_4^{2-}) content, while formation water is characterized by the presence of major cations like Ba^{2+} , Ca^{2+} , Sr^{2+} in elevated concentrations, rendering it saturated with scale-forming components (Figure 1) [7].

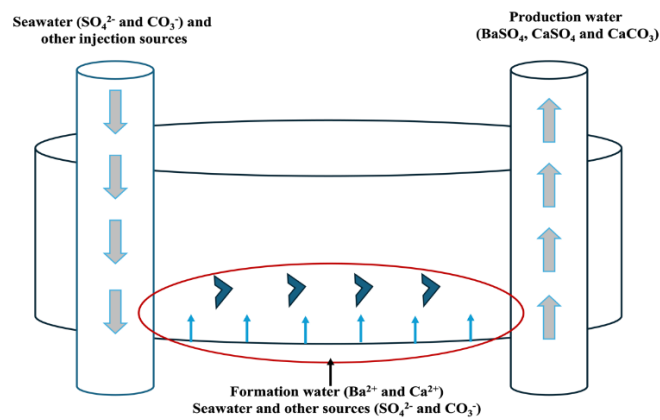


Figure 1 Incompatibility of formation water and seawater

The issue of scale formation represents a significant challenge encountered within the area of the oil and gas industry, exerting considerable influence on the global decline in oil production [7, 11, 12]. In essence, scale is the result of the formation of mineral deposits, which can happen at any stage of oil and gas production in as much as water is present [13]. For instance, scale deposition is more likely to occur in large-volume oil wells that produce water through water injection processes or straight from the reservoir [14]. Sulphate and carbonate scales are the two main types found in the field of oilfield scales. Sulphate scales have the propensity to accumulate in various locations such as reservoirs, perforation intervals, production facilities, pipes, tubing, and so forth. Furthermore, it can clog perforations and impede fluid flow, while the deposition on pipe and tubing walls can reduce the internal diameter, as illustrated in Figure 2. Moreover, the encrustation and impairment of downhole equipment, such as the surface-controlled subsurface safety valve, pose additional challenges. Ultimately, the presence of sulphate scales exacts a toll by inducing a substantial pressure drop within the reservoir, consequently precipitating a sharp decline in oil production [15]. This scenario also fosters material degradation, thereby creating a pathway to unforeseen equipment shutdowns [16]. These complications engender substantial financial repercussions for industries, leading to multimillion-dollar losses annually as a consequence of destruction and decline in production [13].

The approximated international cost attributed to scale-related issues exceeds USD 4 billion on an annual basis [16, 17]. Numerous reported cases underscore the detrimental impact of scaling, particularly sulfate scales, induced by the introduction of seawater to bolster recovery efforts. A noteworthy case study conducted in the Chestnut Field within the North Sea area elucidates a stark decline in oil production from 3800 to 1000 barrels per day within a single month [16]. Another instance of a sharp drop in oil production was recorded in Alba field in the North Sea. The main issue they encountered was the buildup of calcium sulphate scale brought on by inundation with seawater. Thus, in oilfields, determining when seawater breakthrough begins is essential.

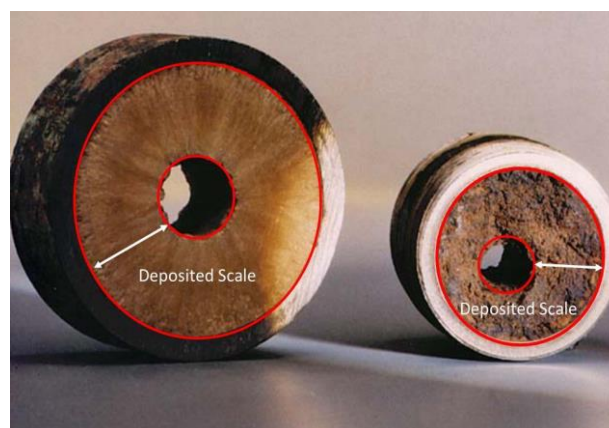


Figure 2 Scale formation in tubing and pipeline

The selection of the most appropriate method is contingent upon the nature of the injected water, with variations observed particularly in the case of seawater injection, a prevalent practice in the industry. Monitoring the amount of SO_4^{2-} present in the produced water enables the determination of seawater breakthrough (SWB) and seawater fraction (SWF) in the system. Given the unique properties of SO_4^{2-} as a natural tracer and its significant role in interacting with cations to form inorganic scales, it emerges as a key focus in the analysis of produced water. The technique involving natural tracers involves a comparative analysis of the ionic

concentrations in the produced water against those present in the formation brine and injected water [13]. Consequently, an elevation in the amount of SO_4^{2-} present within the produced brine signals the influx of seawater into the production system, indicative of a breakthrough event. Such breakthrough occurrences have the potential to trigger sulphate scale deposition in the vicinity of the wellbore or within the topside processing facilities, necessitating prompt interventions to mitigate the risks associated with scaling phenomena.

Numerous analytical techniques are employed in the assessment to determine the amount of SO_4^{2-} within the water that is produced alongside oil. Among the most frequently utilized techniques by operators in the oilfield industry include ion chromatography (IC), gas chromatography-mass spectroscopy (GC-MS), inductively coupled plasma-mass spectroscopy (ICP-MS), and high-pressure liquid chromatography (HPLC). These methods serve as robust instruments for the analysis of oilfield water, supplanting traditional analytical methods such as volumetry and gravimetry, among others [15]. Among the salient features of these methods are automation, sensitivity, repeatability, precision, rapidity, and high matrix tolerance. Unlike other methods, only one contact takes place during the separation procedure [18]. Regrettably, each of these techniques is accompanied by its own set of constraints, with several suffering from reduced accuracy attributable to the presence of dissolved ions or operational costs. For instance, the initial setup cost of IC and HPLC can range between \$15,000 to \$50,000 for a basic system, with high-end models exceeding \$100,000. Also, analysis per sample can be relatively expensive, considering the cost of reagents, calibration standards and instrument maintenance. Conversely, simpler methods like gravimetric and turbidimetric analysis offer lower operational costs, with cost mainly arising from reagents such as BaCl_2 for the precipitation of BaSO_4 and disposable filters. But gravimetry and turbidimetry lack speed, robustness and are prone to errors but can still be effectively used for simpler and less frequent testing. Therefore, it is essential to develop a simple, effective, fast, and affordable method that can be implemented at platforms or laboratories for the oil industry to monitor the produced water's composition in order to detect the beginning of seawater breakthrough.

Procedures such as attenuated total reflectance Fourier transform infrared spectroscopy (ATR-FTIR) warrant consideration for monitoring SO_4^{2-} in produced water due to its rapidity, sensitivity, affordability, and proven efficacy in quantifying anions within solutions for various objectives. As evidenced by a recent examination titled ATR-FTIR detection and quantification of low concentrations of aqueous atomic anions, ATR-FTIR was harnessed as a facile, expeditious, and innovative quantitative means to ascertain the presence of polyatomic anions in aqueous medium at minimal concentrations. The methodology was effectively devised, facilitating the comprehensive study of the anions. Another study carried out using FTIR spectroscopy, combined with ATR, was used to quantitatively and simultaneously determine ion pairs in aqueous solutions. The study investigated salts commonly found in seawater, such as NaCl , KCl , NaBr , KBr , MgCl_2 , CaCl_2 , and Na_2SO_4 , using multivariate data analysis to discriminate and assign spectral information arising from each salt in calibration mixtures [19]. Furthermore, an investigation employed ATR-FTIR spectroscopy to measure ion concentrations in aqueous solutions by analyzing ion-water interactions in the O-H stretching band. Solutions containing various anions, including chloride and phosphate, were prepared at concentrations between 0.5 - 2 M. The method allowed for rapid analysis without pretreatment and showed potential for real-time measurements, with linear regression models achieving high coefficients of determination up to 0.9969 [20].

Given that SO_4^{2-} features an S-O functional group, it consequently yields an IR spectrum within the mid-IR range, thus enabling both qualitative and quantitative analysis. Thus, this investigation was conducted to establish a technique for identifying seawater breakthrough by quantifying the presence of SO_4^{2-} within the produced water utilizing ATR-FTIR. Additionally, finding the detection limit (DL) and quantification limit (QL) for SO_4^{2-} and also investigating whether the existence of supplementary ions affects the precision of the instrument with regards to identifying and quantifying the SO_4^{2-} in the produced water.

2. Materials and methods

2.1 Chemicals preparation of stock solutions

The following salts (Na_2SO_4 , MgSO_4 , $\text{CuSO}_4 \cdot 5\text{H}_2\text{O}$, NaCl , KBr , KCl , NaHCO_3) used in this study were purchased from Kermel, Tianjin, China. Absolute ethanol (95 %) was purchased from Sigma-Aldrich, Burlington MA. Table 1 summarizes the quantities of salts that were solubilized in a 250 ml measuring flask to attain a concentration of 5000 mg/L SO_4^{2-} in each stock solution, in accordance with the ASTM standard procedure [21]. The preparation of the stock solutions was conducted in duplicate. Nine standard solutions with concentrations ranging from 20 to 4000 mg/L were formulated in 25 ml volumetric flasks through additional dilution of each stock solution with deionized water (DW). A total of six stock solutions and 36 standards were prepared in total. This concentration range for the standards was intentionally selected to encompass the anticipated SO_4^{2-} concentration in the samples.

Table 1 Individual Stock solutions

Salt	Conc. (mg/L)	Vol. (ml)	SO_4^{2-} fraction	Mass (g)
Na_2SO_4	5000	250	0.676	1.848
MgSO_4			0.798	1.567
$\text{CuSO}_4 \cdot 5\text{H}_2\text{O}$			0.254	3.249

2.2 Repeatability and reproducibility measurements

To effectively capture and monitor real-time fluctuation in measurements, a repeatability study is often conducted. For this specific procedure, a study of repeatability was conducted on a randomly chosen sample with 5000 mg/L Na_2SO_4 . Ten measurements were made in the same way for this purpose, meaning that the measurand was analysed multiple times. The same instrument, individual and the analyses were performed over a brief timeframe. For reproducibility measurement, in the context of this study, an assessment of within-laboratory reproducibility was conducted on the measurand under investigation [22]. The preparation of stock solutions for generating standards involved the utilization of three distinct salts containing sulfate, namely Na_2SO_4 , $\text{CuSO}_4 \cdot 5\text{H}_2\text{O}$ and MgSO_4 . Each salt was used to prepare three parallel stock solutions for standard production, with the subsequent analyses of these standards being carried out on different days. The evaluation of the mean, SD, and % RSD of the results obtained was documented.

2.3 Preparation of synthetic seawater (SSW) and Draugen formation water (DFM)

Following the standardized procedure outlined in ASTM D1141, solutions of SSW and DFW were meticulously prepared and stored under ambient conditions for future utilization. The composition of seawater, as detailed in Table 2, is primarily constituted by various salts. The salinity of seawater is directly associated with the abundance of dissolved salts, with a reported presence of approximately 7.7% SO_4^{2-} equivalent to around 2700 ppm SO_4^{2-} [21, 23]. Therefore, the following salts were dissolved to achieve the desired salinity. As a point of comparison, Table 2 outlines the salts that make up a specific reservoir water known as draugen, which has a 43% total salt concentration and no SO_4^{2-} present. Draugen is an offshore oil field with associated gas, located at a water depth of 250 m in the southern part of the Norwegian sea [24]. Furthermore, a sample of water from the North Sea near Aberdeen Beach was carefully procured, sealed in an impermeable container, and is intended for application as a representation of natural seawater.

Table 2 Seawater and formation water composition

Salts (seawater)	Mass (g/100 mL)	Salts (draugen)	(g/200 mL)
NaCl	2.453	NaCl	34.70
Na_2SO_4	0.409	CaCl_2	4.900
MgCl_2	0.520	$\text{MgCl}_2 \cdot 6\text{H}_2\text{O}$	2.700
CaCl_2	0.116	KCl	0.400
KCl	0.069	NaHCO_3	0.400
NaHCO_3	0.020	$\text{SrCl}_2 \cdot 6\text{H}_2\text{O}$	0.120
KBr/NaF	0.0103	$\text{BaCl}_2 \cdot 6\text{H}_2\text{O}$	0.061
Total salt	35%	salinity	43%

2.4 FTIR analysis

A diamond crystal FTIR spectrometer, a PerkinElmer brand was employed to conduct the analysis. The configuration of the instrument is stated in Table 3. The same methodology was applied to analyze the remaining samples. It is noteworthy that instead of the traditional transmittance against wavenumber, absorbance was graphed against wavenumber (cm^{-1}). This selection was made due to the emphasis on quantification in this study. Peak height and area in an absorbance spectrum are directly correlated with concentration, according to Beer Lambert's law [25]. Contrarily, % transmittance is more suitable for qualitative rather than quantitative analysis. Firstly, ethanol was used to clean the crystal then a drop of D.W water was gently placed on the hotspot where the analysis was done and the water's IR spectrum was saved as the background. After giving the crystal another thorough cleaning, the samples were cautiously placed on it one by one. Following the acquisition of spectra for every sample, a peak was seen at around 1100 cm^{-1} . This peak is indicative of the S-O stretching vibration attributed to SO_4^{2-} [26]. By merely combining the height of the peak and the baseline endpoints, the area under the peak was found and carefully documented. It is worth noting that the same start and endpoint for each S-O peak (1210 cm^{-1} to 998 cm^{-1}) was used throughout the peak area integration. Figure 3 shows the picture of the ATR-FTIR setup while Figure 4 depicts the schematic illustration of the procedure.

Table 3 ATR-FTIR operating condition all sample analysis

X coordinate	Wavenumber cm^{-1}
Y coordinate	Absorbance
Range	4000 - 400
Data Resolution	2 cm^{-1}
Run Interval	0.5
Sample scan	32
Background scan	16
Scan speed	0.2



Figure 3 ATR-FTIR setup for the analysis

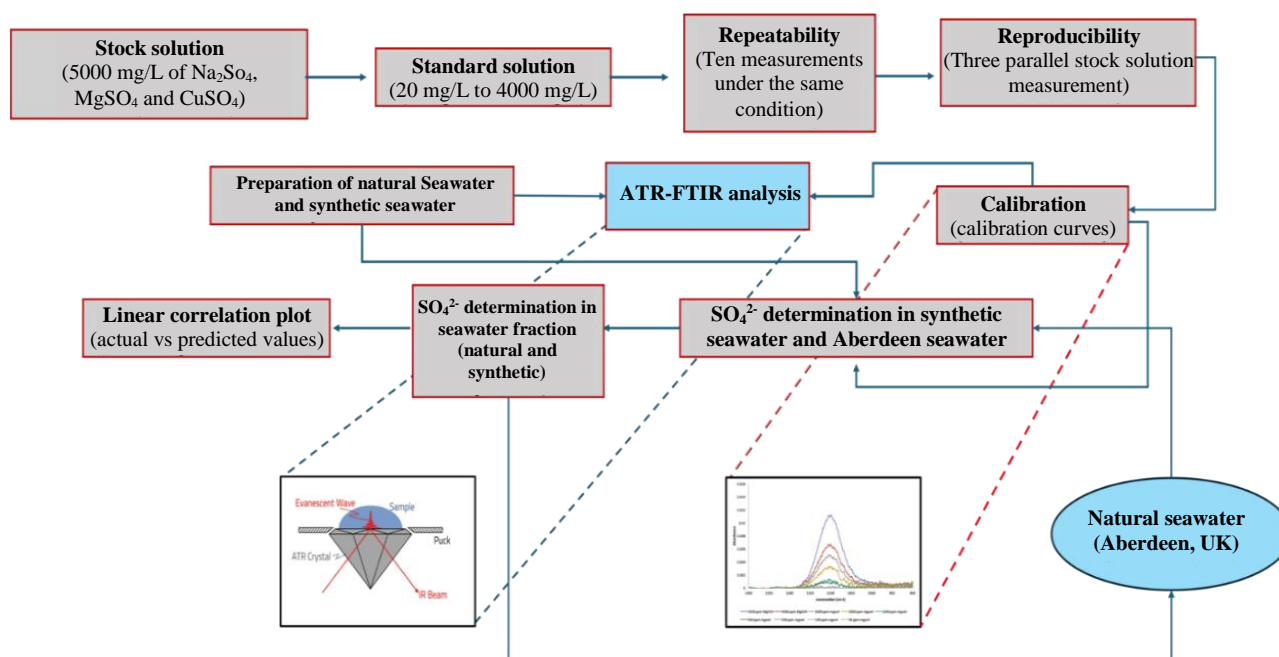


Figure 4 Flowchart for the experimental procedures, analysis methods, and calibration using ATR-FTIR

3. Results and discussion

3.1 Method validation

3.1.1 Repeatability measurement

Repeatability, a crucial concept in measurement science, pertains to the reliability of measurements conducted using a specific method. The consistency and dependability of the results obtained by the instrument are key considerations in assessing repeatability. It is highly preferable that the instrument yields consistent outcomes when subjected to repeated analyses [22]. This preference is rooted in the fact that all measurement instruments inherently possess a degree of random error, which in turn contributes to variability in the measurements. The meticulous examination of the SD, coefficient of repeatability coefficient, and % RSD associated with the measurements reveals remarkably small values, indicating a high level of confidence in the results derived through this analytical method as depicted in Table 4. This high level of statistical certainty suggests that the results are not merely artefacts of the measurement process itself. Consequently, based on the outcomes and the aforementioned observations, FTIR spectroscopy emerges as a dependable and accurate analytical technique.

Table 4 Data from repeatability measurement

Peak area of 5000 mg/L Na ₂ SO ₄	mean	S.D (±)	Coefficient of repeatability	% RSD
0.64	0.646	0.009	0.016	8.7E ⁻⁰³ %
0.64				
0.65				
0.64				
0.65				
0.66				
0.64				
0.66				
0.64				
0.64				

3.1.2 Reproducibility

Reproducibility, a fundamental aspect of scientific inquiry, refers to the capacity of a study to be reproduced or replicated, either by the original researcher or by others. The determination of reproducibility holds significant importance in research endeavors. Table 5 presents the evaluation of the mean, SD, and % RSD of the results obtained. Despite the variations in the source of standards, the analytical results exhibited remarkable consistency. The peak's location at 1100 cm⁻¹ and the peak regions that were similar between measurements made at the same concentrations further support the accuracy of the findings. A high degree of agreement between measurements made under various conditions is indicated by the very small standard deviation and percentage RSD readings, with a maximum uncertainty of 5.5%. This further explains that a repeat of the experiment would probably also give a result in the interval 94.5 < x < 105.5.

Table 5 Data from reproducibility measurement

Conc. (mg/L)	CuSO ₄ .5H ₂ O			MgSO ₄			Na ₂ SO ₄			overall mean	overall STD	overall %RSD
	mean	STD	RSD	mean	STD	RSD	mean	S.D	RSD			
5000	0.650	1.010	0.015	0.640	0.010	0.016	0.643	0.006	0.009	0.644	0.005	0.800
4000	0.537	0.600	0.011	0.520	0.020	0.038	0.530	0.000	0.000	0.529	0.009	1.601
3000	0.383	0.600	0.015	0.360	0.030	0.083	0.377	0.006	0.015	0.373	0.012	3.202
2000	0.263	1.22	0.044	0.237	0.006	0.024	0.243	0.006	0.024	0.248	0.014	5.504
1000	0.133	0.600	0.043	0.123	0.006	0.047	0.143	0.006	0.040	0.133	0.010	3.502
500	0.073	0.600	0.079	0.070	0.010	0.143	0.070	0.010	0.143	0.071	2.0E ⁻³	2.402
200	0.043	0.600	0.133	0.033	0.006	0.173	0.043	0.006	0.133	0.040	6.0E ⁻³	1.440
100	0.021	0.600	0.247	0.020	0.00	0.00	0.020	0.00	0.00	0.021	2.0E ⁻³	4.190
50	0.010	0.00	0.00	0.010	0.00	0.00	0.010	0.00	0.00	0.010	0.00	0.00
20	<DL	0.00	0.00	<DL	0.00	0.00	<DL	0.00	0.00	<DL	0.00	0.00

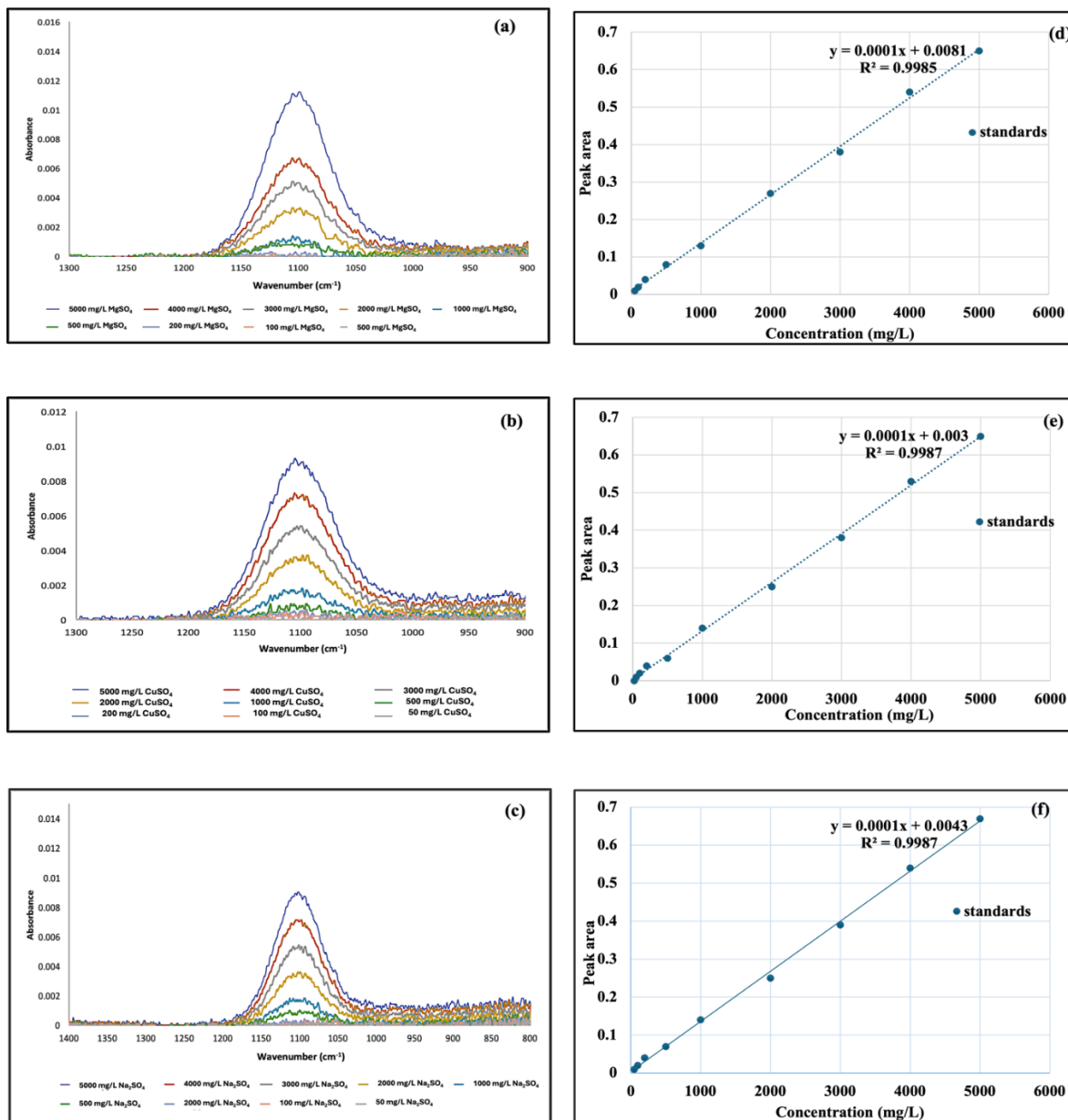


Figure 5 stacked IR spectra for (a) MgSO₄, (b) CUSO₄ (c) Na₂SO₄ and Calibration graph for (d) MgSO₄, (e) CuSO₄.5H₂O (f) Na₂SO₄

3.2 Calibration

Furthermore, three distinct calibration curves were generated from each parallel sample, with the most suitable curve being selected for illustration alongside its corresponding IR spectrum, which elucidates the S-O peaks that resulted from each of the standards analysis. Peak areas were measured for each standard by integrating the peak of interest. The resulting data was then used to create a calibration curve that shows the peak area as a function of concentration. Figure 5 displays the spectra and calibration graph for the Na₂SO₄, MgSO₄, and CuSO₄.5H₂O standards, respectively. The peaks demonstrate a range of quality and sharpness, varying from

highly defined and dominant peaks at elevated concentrations to poorly delineated peaks at reduced concentrations. Each calibration curve presented exhibits a regression factor (R^2) that approaches unity, which is deemed satisfactory [27]. This observation serves as an indication that the calibration employing FTIR is indeed appropriate [24].

The approximated DL and QL for SO_4^{2-} in the standards were determined to be 50 mg/L and 100 mg/L, respectively. The reason for this determination is that, at 50 mg/L, the S-O peak's absorbance was visible but was incapable of being effectively integrated to yield an accurate peak area; in contrast, at 100 mg/L, the peak was more clearly defined, making integration and recording the peak area easier. A concentration of 20 mg/L was found to be below the DL for SO_4^{2-} , necessitating its exclusion from the calibration curve due to the lack of any identifiable peaks. The utilization of other advanced analytical methods previously referenced, such as IC and HPLC, enables the detection of ions well below the 20 mg/L threshold, extending to the parts per billion level [18]. Despite the exceptional sensitivity exhibited by these instruments, there exist certain trade-offs that must be considered during analysis, including operational costs, time allocation for analysis, and the level of labor intensity involved.

3.3 Impact of the addition of supplementary ions on the analysis

One objective of this investigation was to ascertain whether the incorporation of additional ions within the aqueous medium affects the instrument's sensitivity regarding the detection and quantification of the concentration of SO_4^{2-} . An example of an infrared spectrum for seawater containing two components ($\text{NaCl} + \text{Na}_2\text{SO}_4$) is shown in Figure 6 (a). The unique water band seen in the 3600–3200 cm^{-1} spectral range is caused by NaCl presence in the aqueous medium. When the solution contains alkali chloride salts (NaCl , KCl , or RbCl) and is subjected to FTIR, the water band exhibits a sinusoidal profile rather than the typical broad water band, which is centred around 3400 cm^{-1} . The existence of non-bonded free O-H groups in the aqueous medium is the cause of this unusual water peak [28]. In contrast to the cynical peak at roughly 3200 cm^{-1} , which is connected with a decrease in the hydrogen-bonded water network because of the existence of free Cl groups, the significant positive peak seen around 3400 cm^{-1} is correlated with hydrogen-bonded water molecules. Even when water is used as a standard, the water band may show a positive-negative peak in the spectrum if hydrogen bonding is reduced. As seen in Figure 6 (b), the S-O peak at 1100 cm^{-1} is unaffected by the presence of this peak. No changes in peak area, peak position, or even an overlap were seen in that spectral region, even in the presence of increased complexity in the aqueous solution as a result of the addition of various components during the synthesis of seawater as evidenced in Table 6. The results indicate that the sensitivity of the device in measuring the concentration of SO_4^{2-} is unaffected by the existence of supplementary ions, particularly anions like HCO_3^- and Cl^- in saltwater. Thus, even with the additional complexity brought forth by the existence of various ions, the peak associated with sulfate can still be accurately identified and quantified.

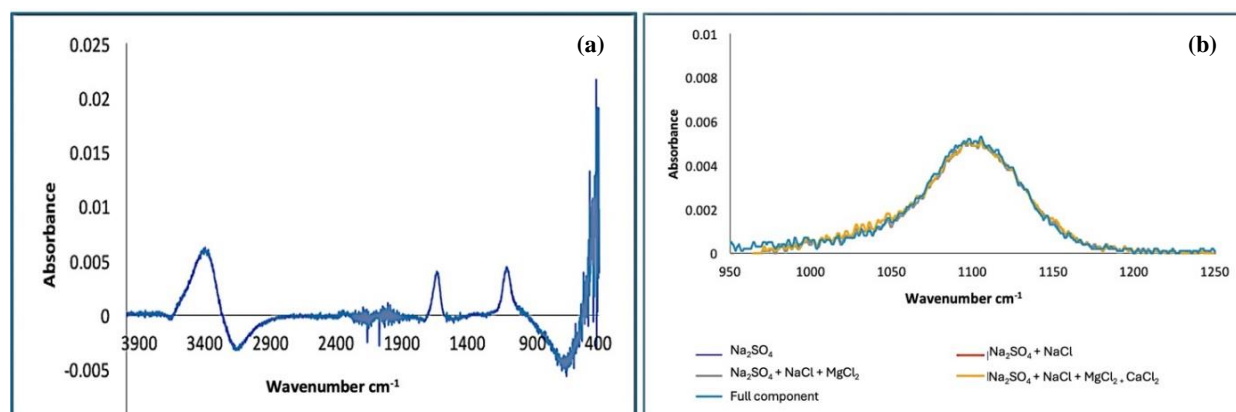


Figure 6 IR spectrum of (a) $\text{Na}_2\text{SO}_4 + \text{NaCl}$ and (b) Sulfate peaks with inclusion of other salts

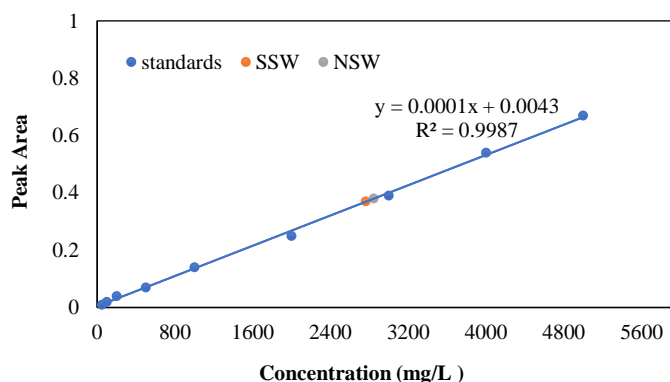
Ionic components particularly anions in produced water were tracked using IC in a recent work on the application of IC to oilfield water analysis [29]. A non-suppressed conductivity detector was used to identify cations, and a suppressed conductivity detector was used to identify anions. The examination of ions, in particular anions, presented difficulties since offshore oil well water has a high Cl^- content and a complicated matrix. Extensive treatment and multiple injections were necessary prior to analysis, and the produced water had to be significantly diluted (at least 1000x) because of its high conductivity stemming from the elevated Cl^- levels. Initially, only Cl^- was detectable in the analysis, with all other anions present in the produced water remaining in the baseline field and undetectable. Consequently, the Cl^- had to be eliminated first, enabling the accurate measurement of other anions such as SO_4^{2-} and NO_3^- . The demonstration illustrates that the existence of several ions in the aqueous solution has the potential to influence the measurement of the ions targeted for determination through IC, particularly in water samples exhibiting exceptionally high salinity levels. It is noteworthy that not only ions but also the existence of hydrocarbons and artificially introduced compounds can introduce significant interferences during the analytical process. Furthermore, in the context of water with elevated Cl^- concentrations, it is crucial to manage the treatment procedures effectively to prevent the column from reaching its capacity limit. Failure to address this issue adequately may result in substandard chromatographic performance, manifesting as peak suppression or exceeding the linear calibration range, consequently yielding inaccurate analytical outcomes. This observation underscores the necessity for meticulous handling of samples to ensure the reliability of IC analysis. In contrast, findings from FTIR experiments revealed that the elevated Cl^- levels in the water sample did not yield any discernible impact on the accurate identification and quantification of SO_4^{2-} . The absence of any noticeable changes in the spectral peaks associated with ions indicates the robustness of FTIR in such scenarios. Moreover, the portability, user-friendly operation, and cost-effectiveness of FTIR instrumentation position it as a promising tool for facilitating concurrent monitoring of SO_4^{2-} in-situ within produced water samples, without encountering significant operational challenges. Because it eliminates the time lag involved in transferring samples to off-site laboratories for examination utilising techniques such as HPLC, ICP and GC spectroscopy, in-situ analysis of generated water calls for important significance.

Table 6 Data from S-O peaks with the addition of different salts

Salts	Peak area at 1100 cm ⁻¹
Na ₂ SO ₄	0.380
Na ₂ SO ₄ + NaCl	0.376
Na ₂ SO ₄ + NaCl + MgCl ₂ .6H ₂ O	0.375
Na ₂ SO ₄ + NaCl + MgCl ₂ .6H ₂ O + CaCl ₂	0.381
Na ₂ SO ₄ + NaCl + MgCl ₂ .6H ₂ O + CaCl ₂ + NaHCO ₃	0.376
Full components of seawater	0.376

3.4 SO₄²⁻ determination in SSW and NSW

The calibration graph for Na₂SO₄ that was previously shown was employed in calculating the SO₄²⁻ concentration in both SSW and NSW using the calibration curve equation. The Na₂SO₄ calibration curve was selected for the study because all three of the calibration curves shown above demonstrated exceptional linearity (Figure 7). As previously stated, the concentration of SO₄²⁻ in the SSW is anticipated to be around 2700 mg/L, while the SO₄²⁻ concentration determined using the calibration graph yielded 2776 mg/L. In addition, the measured SO₄²⁻ concentration in NSW from the shores of Aberdeen was discovered to be 2834 mg/L, slightly higher than the expected value of approximately 2800 mg/L as shown in Table 7. There are geographical variations in saltwater salinity that can be seen, especially in places where water is in fluxed [30]. For example, the average total salinity of North seawater is stated to be between 34 - 35‰, of which 8‰ is attributable exclusively to SO₄²⁻. This means that 8% of the total salt content is equivalent to 2800 mg/L of SO₄²⁻ [28]. Despite the little variation in values, the close agreement between the observed and expected SO₄²⁻ concentrations shows the validity of FTIR for quantitative analysis, and the limited impact of other ions on these measurements implies low matrix interference in FTIR analysis.

**Figure 7** Calibration graph for Na₂SO₄ with SO₄²⁻ concentration in both SSW and NSW**Table 7** SO₄²⁻ concentration in water samples

Sample type	Peak area	Conc. (mg/L)
Synthesized SW	0.376	2776
Aberdeen beach SW	0.381	2834

The efficiency of this method surpasses that of other contemporary techniques such as IC and classical methods like gravimetric analysis, significantly reducing the analysis time. The generation of a spectrum takes less than two minutes while determining the peak area or peak height of the analyte of interest from the spectrum requires less than a minute as well. Additionally, FTIR is promptly available for the subsequent sample analysis following a simple clean-up procedure with a ball of cotton wool. Conversely, an approach like IC demands a considerable amount of time due to multiple analysis steps involving injection, ion separation, and chromatograph generation, especially for the analysis of anions and cations at parts per billion levels [31].

3.5 Determination of SO₄²⁻ in seawater fraction

The seawater Fraction (SWF) denotes the proportion of seawater present in the produced water. Assessing the SWF in produced water is crucial for anticipating scale-related issues, evaluating their severity, and devising appropriate mitigation strategies. A salinity of 43,000 mg/L on average and free of SO₄²⁻ was obtained from artificial draugen formation water, which was used as a reference in this investigation. The absence of SO₄²⁻ in the water can be observed from the spectrum as no absorbance around the 1100 cm⁻¹ was observed as seen in Figure 8 (a) and (b). By mixing different portions of formation water and seawater, the SWF was established. Both SSW and NSW were analysed, and the peak area of each proportion was determined by integrating the S-O peak, which was found in the spectrum at 1100 cm⁻¹. The SO₄²⁻ concentration in the SWF was measured using the same Na₂SO₄ calibration curve that was used to ascertain the concentration of SO₄²⁻ in both seawaters. Table 8, Figure 9 (a) and (b) display the results for synthetic SWF, and Table 8, Figure 9 (c) and (d) display the results for natural (Aberdeen) SWF.

The observed discrepancy in the range of higher levels of produced water is demonstrated by the data points that do not align as predicted; as a result, the line does not intersect the origin, in contrast to the calibration curves previously observed. When preparing seawater fractions, it is essential to use an even quantity of seawater with a known concentration of SO₄²⁻ when altering the formation of water's composition. This helps to ascertain the impact of the presence of other ions at elevated concentrations compared to that of

seawater, such as Cl, for the accurate quantification of SO_4^{2-} . Furthermore, the results obtained earlier indicate that the approximated DL for SO_4^{2-} in both synthetic seawater fraction (SSWF) and natural seawater fraction (NSWF) stands at 100 mg/L for each, corresponding to a composition of 5% seawater and 95% formation water. On the other hand, QL for SSWF and NSWF is approximated to be 414 mg/L and 500 mg/L, respectively, aligning with compositions of 10% seawater and 90% formation water. This implies that FTIR spectroscopy is capable of detecting SO_4^{2-} at concentrations as low as 5% seawater in the produced brine. The utilization of scale modelling software can aid in forecasting the threshold concentration at which the presence of SO_4^{2-} becomes problematic, revealing it to be above the LOD of FTIR. In such cases, the initiation of a breakthrough is not anticipated to pose a concern. However, if the anticipated concentration of SO_4^{2-} falls below that detectable by FTIR, complementary methodologies must be employed in conjunction with FTIR to identify the onset of breakthrough.

Given the cost-efficient operational nature of ATR-FTIR spectroscopy, characterized by the absence of consumables such as reagents, chemicals, or energy sources, analytical procedures can be executed promptly and economically. This expeditious approach not only enables the prompt detection of breakthrough events but also facilitates the implementation of effective scale mitigation strategies in a timely fashion. The affordability and efficiency of FTIR instrumentation present a compelling case for its utilization in the swift and accurate determination of water quality parameters, underscoring its potential to revolutionize analytical practices in water treatment and environmental monitoring applications.

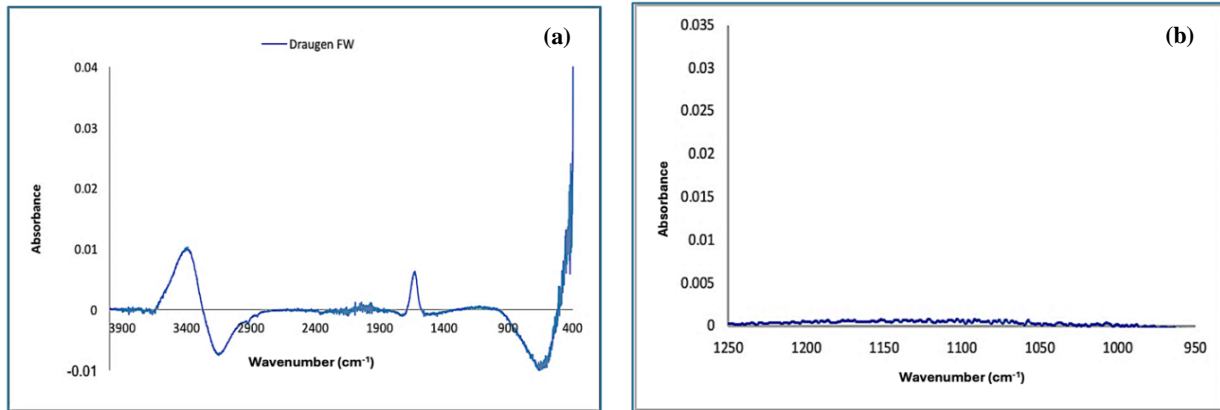


Figure 8 (a) Full DFW IR spectrum and (b) detailed examination of DFW IR spectrum

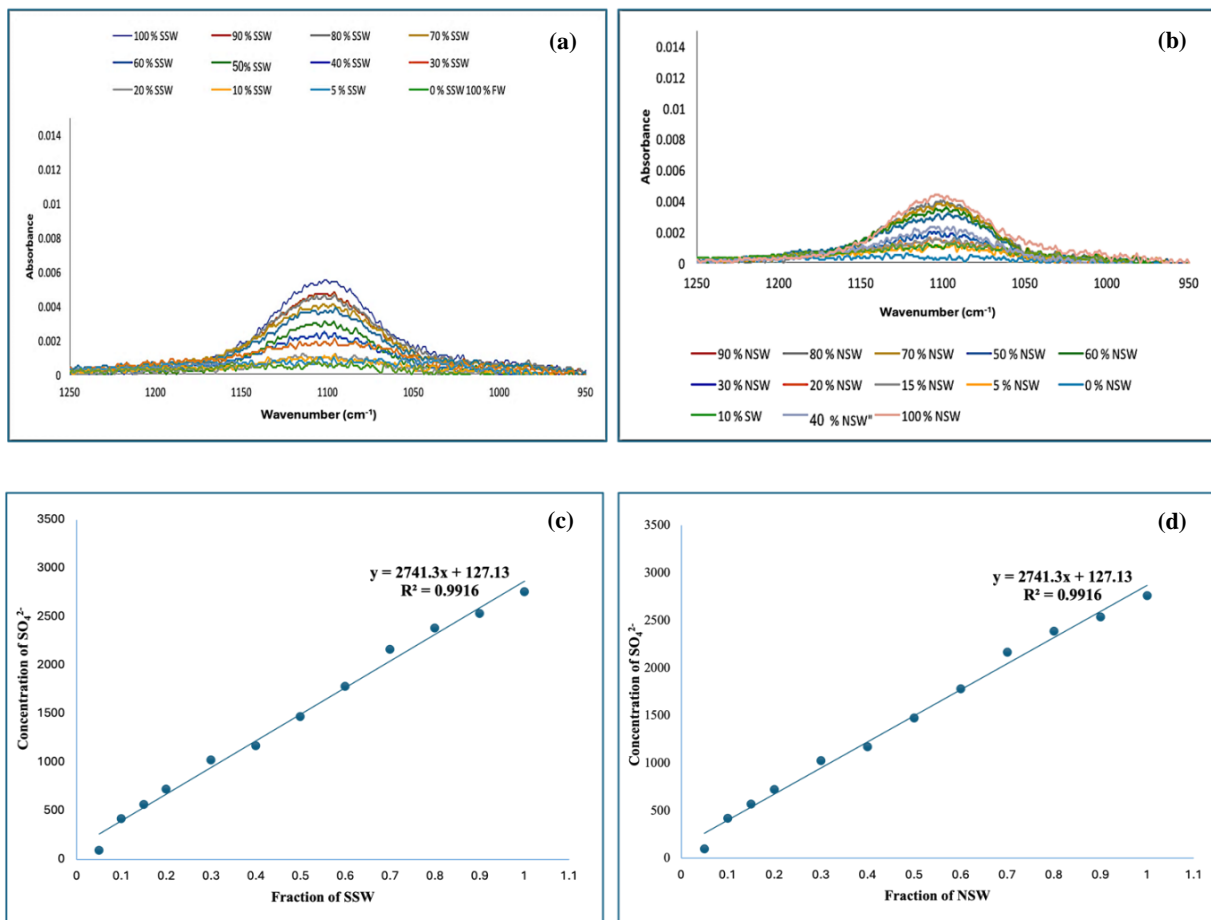


Figure 9 (a) Stacked IR spectra of SSWF, (b) Stacked IR spectra of NSWF, (c) graph of SO_4^{2-} concentration vs NSWF and (d) graph of SO_4^{2-} concentration vs SSWF

Table 8 Peak area and concentration of SO₄²⁻ in SSWF and NSWF

SSWF	Concentration(mg/L)	Peak area	NSWF	Concentration (mg/L)	Peak area
0.05	100	0.02	0.05	100	0.02
0.1	414	0.06	0.1	500	0.07
0.15	576	0.08	0.15	656	0.09
0.2	722	0.10	0.2	804	0.11
0.3	1022	0.14	0.3	1032	0.14
0.4	1180	0.16	0.4	1172	0.17
0.5	1476	0.20	0.5	1490	0.20
0.6	1780	0.24	0.6	1786	0.24
0.7	2236	0.30	0.7	2080	0.28
0.8	2392	0.32	0.8	2392	0.32
0.9	2540	0.35	0.9	2610	0.35
1	2776	0.37	1	2834	0.38

3.6 Linear correlation plot

Table 9 and Figure 10 present a linear reciprocity plot that was obtained by comparing the measured and actual concentrations of SO₄²⁻ in NSW and SSW to improve the methodology for computing SO₄²⁻ within the SWF derived from the produced water. Linear reciprocity plots serve as effective tools for evaluating the consistency of correlations within a dataset and also serve to validate the accuracy of the measurement procedures being undertaken. The plots depicted above illustrate a strong linear relationship between the variables, with a coefficient of determination calculated to be 0.9946 for synthetic SWF and 0.9946 for natural NSWF. Examination of the plots reveals that the data points closely align with the regression line, despite the measured concentration values being slightly elevated compared to the actual concentrations. This observation suggests a robust correlation between the two datasets as evidenced by the plots. Notably, due to discrepancies particularly evident at higher fractions of produced water, the regression lines for both SSWF and NSWF do not intersect at zero.

Table 9 Actual vs measured concentration of sulfate ion in NSWF

Actual concentration	Measured concentration
2800	2834
2520	2610
2240	2394
1960	2084
1680	1786
1400	1490
1120	1170
840	970
560	710
420	405
280	180
140	100

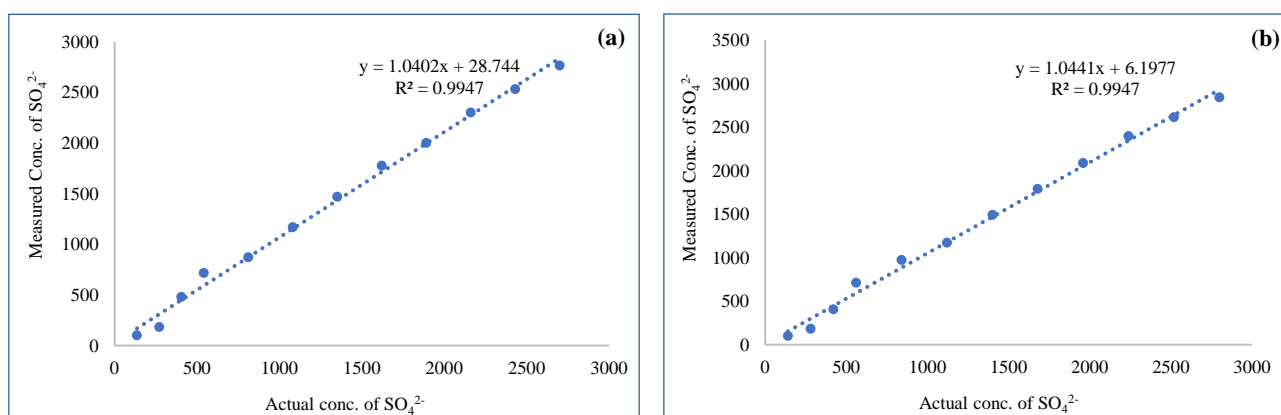


Figure 10 (a) Measured vs actual SSWF plot and (b) measured vs actual NSWF plot

4. Conclusion

An innovative and efficient approach utilizing ATR-FTIR spectroscopy has been successfully devised for the determination of seawater breakthrough. The investigation yielded valuable findings, indicating that the DL for SO₄²⁻ in the calibration standards stands at 50 mg/L, with the QL set at 100 mg/L. The existence of supplementary ions within the water matrix does not compromise the precision of the instruments when quantifying SO₄²⁻. The estimated concentrations of SO₄²⁻ in SSW and NSW were determined to be 2776 mg/L and 2834 mg/L, respectively. Moreover, the DL for SO₄²⁻ in both synthetic SWF as well as natural SWF is established at

100 mg/L, while the QL for SO_4^{2-} in SSWF and NSWF are identified as 414 mg/L and 500 mg/L, respectively. The estimated DL for SO_4^{2-} in both SSWF and NSWF was found at 100 mg/L for each, corresponding to a composition of 5% seawater and 95% formation water. Conversely, QL for SSWF and NSWF is approximated to be 414 mg/L and 500 mg/L, respectively, aligning with compositions of 10% seawater and 90% formation water. It is noteworthy that the linear correlation plots demonstrate a strong relationship between the actual and measured concentrations of SO_4^{2-} in SSWF as well as NSWF, revealing correlation coefficients of 0.9946 for both plots. Even though FTIR may not exhibit the same level of sensitivity as other analytical approaches such as IC and ICP, it remains a dependable and precise method for analysis. The capability for conducting real-time analysis efficiently within a relatively brief timeframe further underscores the utility of FTIR in such contexts. The obviation of extensive sample preparation emerges as a distinct advantage, especially evident in the context of ATR-FTIR spectroscopy, where merely a small water droplet proves sufficient for analysis. Furthermore, the employment of ATR-FTIR overcomes delays imposed by limited sampling of water due to cost considerations and logistical challenges engendering difficulties in promptly identifying the onset of seawater breakthrough, potentially resulting in delays in implementing requisite scale mitigation measures.

5. Acknowledgement

The research reported in this publication expands upon the findings of the master thesis titled "Developing a method to follow the breakthrough of seawater using FTIR spectroscopy which was completed at the University of Aberdeen, United Kingdom. This manuscript contains unique insights and enlarged analysis not available anywhere.

6. References

- [1] Rasheed HA, Adeleke A, Nzerem P, Ajayi O, Ikubanni P, Yahya AM. A review on the use of carboxymethyl cellulose in oil and gas field operations. *Cellulose*. 2023;30:9899-924.
- [2] Zhao X, Zhu S. Prediction of water breakthrough time for oil wells in low-permeability bottom water reservoirs with barrier. *Pet Explor Dev*. 2012;39(4):504-7.
- [3] Amarfio EM, Brobbey O. Evaluation of various water flooding patterns in the Kube field. *Int J Petroleum Petrochemical Eng*. 2019;5(2):1-8.
- [4] Ayoub MA, Shabib-Asl A, AbdellahiZein AM, Elraies KA, Bin Mohdasaad I. Recovery optimization of an oil reservoir by water flooding under different scenarios; a simulation approach. *Res J Appl Sci Eng Technol*. 2015;10(4):357-72.
- [5] Abbasi S, Farahani H, Shahrabadi A. Water injection process monitoring in injection wells and its effect on the production wells. The 1st international conference on oil gas, petrochemical and power plants; 2012 Jul 16; Tehran, Iran.
- [6] Amiri M, Moghadasi J, Jamialahmadi M, Shahri MP. The study of calcium sulphate scale formation during water injection in Iranian oil fields at different pressures. *Energy Sources A: Recovery Util Environ Eff*. 2013;35(7):648-58.
- [7] Taha A, Amani M. Water chemistry in oil and gas operations: scales properties and composition. *Int J Org Chem (Irvine)*. 2019;9(3):130-41.
- [8] McCartney R, Moldrheim E, Fleming N. Detection and quantification of Utsira formation water in production wells of the Oseberg Sør Field and impact on scale management. The 21st International Oil Field Chemistry Symposium; 2010 Mar 15-17; Geilo, Norway. p. 1-30.
- [9] McCartney RA. Conditions under which anhydrite precipitation can occur in oil reservoirs as a result of seawater injection. The 19th International Oilfield Chemistry Symposium; 2008 Mar 9-12; Geilo, Norway. p. 1-25.
- [10] Sukhija BS, Reddy DV, Nagabhushanam P, Patil DJ, Hussain S, inventors. Process utilizing natural carbon-13 isotope for identification of early breakthrough of injection water in oil wells. United State: US Patent US8283173B2. 2012 Oct 9.
- [11] McCartney RA, Melvin K, Wright R, Sørhaug E. Seawater injection into reservoirs with ion exchange properties and high sulphate scaling tendencies: modelling of reactions and implications for scale management, with specific application to the Gyda Field. The 18th International Oilfield Chemistry Symposium; 2007 Mar 26-28; Geilo, Norway. p. 1-23.
- [12] Ephraim O, Awajjogak U. Determining the rates for scale formation in oil wells. *Int J Eng Res Appl*. 2016;6(9):62-6.
- [13] Patel J, Nagar A. Oil field scale in petroleum industry. *Int J Innov Res Eng Manag*. 2022;9(2):288-93.
- [14] Yuan M, Todd AC, Sorbie KS. Sulphate scale precipitation arising from seawater injection: a prediction study. *Mar Pet Geol*. 1994;11(1):24-30.
- [15] El-Said M, Ramzi M, Abdel-Moghny T. Analysis of oilfield waters by ion chromatography to determine the composition of scale deposition. *Desalination*. 2009;249(2):748-56.
- [16] Al Rawahi YM, Shaik F, Nageswara Rao L. Studies on scale deposition in oil industries & their control. *Int J Innov Res Sci Technol*. 2017;3(12):152-67.
- [17] Bin Merdiah AB, Mohd Yassin AA. Study of scale formation in oil reservoir during water injection-a review. Marine science and Technology seminar; 2007 Feb 22-23; Kuala Lumpur, Malaysia. p. 1-7.
- [18] Xu Q, Xu C, Wang Y, Zhang W, Jin L, Tanaka K, et al. Amperometric detection studies of poly-o-phenylenediamine film for the determination of electro inactive anions in ion-exclusion chromatography. *Analyst*. 2000;125(8):1453-7.
- [19] Rauh F, Mizaikoff B. Simultaneous quantification of ion pairs in water via infrared attenuated total reflection spectroscopy. *Anal Methods*. 2016;8(10):2164-9.
- [20] Baek SH, Yun J, Lee SH, Lee HW, Kwon Y, Park KR, et al. Real-time analysis and prediction method of ion concentration using the effect of O-H stretching bands in aqueous solutions based on ATR-FTIR spectroscopy. *RSC Adv*. 2024;14(28):20073-80.
- [21] Speight JG. Chapter 4 - Reservoir Fluids. In: Speight JG, editor. *Introduction to Enhanced Recovery Methods for Heavy Oil and Tar Sands*. Cambridge: Elsevier; 2016. p. 123-75.
- [22] Nicholson G, Holmes C. A note on statistical repeatability and study design for high-throughput assays. *Stat Med*. 2017;36(5):790-8.
- [23] Angelis MD. Major Ions in Seawater. In: Lehr JH, Keeley J, editors. *Water Encyclopedia*. Wiley; 2005. p. 159-60.
- [24] Reinholdtsen B. Draugen field development: the role of gravity drainage and horizontal wells. *Pet Geosci*. 1996;2(3):249-58.
- [25] Mayerhöfer TG, Pipa AV, Popp J. Beer's law-why integrated absorbance depends linearly on concentration. *ChemPhysChem*. 2019;20(21):2748-53.

- [26] Nandiyanto ABD, Oktiani R, Ragadhita R. How to read and interpret FTIR spectroscopy of organic material. *Indonesian J Sci Technol.* 2019;4(1):97-118.
- [27] Rasheed HA, Adeleke AA, Nzerem P, Olosho AI, Ogedengbe TS, Jesuloluwa S. Isolation, characterization and response surface method optimization of cellulose from hybridized agricultural wastes. *Sci Rep.* 2024;14(1):14310.
- [28] Suárez L, García R, Riera FA, Díez MA. ATR-FTIR spectroscopy for the determination of Na₄EDTA in detergent aqueous solutions. *Talanta.* 2013;115:652-6.
- [29] Altundag H, Agar S, Altıntig E, Ates A, Sivrikaya S. Use of ion chromatography method on the determination of some anions in the water collected from Sakarya, Turkey. *J Chem Metrol.* 2019;13(1):14-20.
- [30] Heath MR, Henderson EW, Slesser G, Woodward EMS. High salinity in North Sea. *Nature.* 1991;352:116.
- [31] Tomić T, Nasipak NU. Application of ion chromatography in oilfield water analysis. *Holistic Approach Environ.* 2012;2:41-8.